Journal of Sound and Vibration 325 (2009) 816–834

Contents lists available at ScienceDirect

Journal of Sound and Vibration

journal homepage: www.elsevier.com/locate/jsvi

Dynamic response of a pair of elliptic tunnels embedded in a poroelastic medium

Xiang-Lian Zhou [a,*], Jian-Hua Wang [a], Ling-Fa Jiang [b]

[a] Department of Civil Engineering, Shanghai Jiaotong University, Shanghai 200240, PR China
[b] Institute of Rock and Soil Mechanics, The Chinese Academy of Science, Wuhan 430071, PR China

ARTICLE INFO

Article history:
Received 22 May 2008
Received in revised form
2 April 2009
Accepted 3 April 2009
Handling Editor: L.G. Tham
Available online 8 May 2009

ABSTRACT

In this paper, a semi-analytical method is developed to solve the dynamic response of a pair of parallel elliptic tunnels embedded in an infinite poroelastic medium. The surrounding poroelastic medium of tunnels is described by Biot's poroelastic theory, while the tunnels are treated as a single-phase elastic medium. By introducing potentials, the governing equations are reduced to Helmholtz equations. The series solutions of the Helmholtz equations are obtained by the wave function expansion method. The surrounding poroelastic medium and the tunnels are coupled together via the stresses and the displacements continuation conditions. Numerical results demonstrate that the dimensionless wavenumber, distance between two tunnels, elliptic ratio and thickness of liner have a considerable influence on the dynamic response of the tunnels and the poroelastic medium.

1. Introduction

Tunnel in soft ground is an increasingly common geotechnical activity for construction of urban transportation or water management facility in many large cities around the world. For this reason, numerous researcher use various methods to investigate this problem. In practice, most underground soils must use various liners to support tunnels. Therefore, a better understanding of the dynamic interaction between the tunnel and its surrounding media subjected to seismic wave is desirable in earthquake engineering and civil engineering.

Numerous investigations for seismic response of cavity or tunnel have been carried out in the past years. Among these, Zitron [1] dealt with the multiple scattering of plane elastic wave by two arbitrary cylinders in a homogeneous medium. Glazanov and Shenderov [2] studied the plane wave scattering by a cylindrical cavity in an isotropic elastic medium. Varadan [3] studied the scattering of *P*, *SV* and *SH* waves by an elliptic cavity using the scattering matrix approach. Lee and Trifunac [4] analyzed the two-dimensional scattering and diffraction of *SH* wave by a circular tunnel in a homogeneous elastic half-space using the series solution method. Chen [5] analyzed the dynamic response of a circular lined tunnel subject to *SH* wave using the wave function expansion method. Fotieva [6] studied the two parallel circular tunnels subjected to the compressional and the shear waves. Sancar and Pao [7] gave the solution for the scattering of plane harmonic wave by two cylindrical cavities in an elastic solid using the eigenfunction expansion method. Datta et al. [8] studied the dynamic stress and the displacement around a cylindrical cavity in an elastic medium using the combined finite element method and the eigenfunction expansion method. Zeng and Cakmak [9] investigated the scattering of *SH*

* Corresponding author.
E-mail addresses: zhouxl@sjtu.edu.cn, zhoux199@hotmail.com (X.-L. Zhou).

0022-460X/$ - see front matter © 2009 Elsevier Ltd. All rights reserved.
doi:10.1016/j.jsv.2009.04.001

wave by multiple cavities in both an infinite and a half-space using the series expansion method. Moeen-Vaziri and Trifunac [10] solved the problem of the scattering and diffraction of *SH* wave by a cylindrical canal of arbitrary shape in an elastic half-space using the boundary element method. Providakis et al. [11] studied the stress concentration around multiple circular cavities using the boundary element method and the Laplace transform method. Shi et al. [12] studied the interaction of *SH* wave and a lined in an anisotropic medium using the conformal mapping method and the wave function expansion method. Stamos et al. [13] studied the three-dimensional dynamic response of the long-lined tunnel in a half-space using the boundary element method. Davis et al. [14] investigated the transverse response of an underground cylindrical cavity subjected to incident shear wave using the Fourier–Bessel series method. Eisenberger and Efraim [15] studied the dynamic response of a piecewise tunnel consists of several liner pieces and connecting joints using the curved beam theory. Okumura et al. [16] investigated the dynamic interaction of the twin circular tunnels subjected to an incident *SV* wave using the two-dimensional finite element method. Moore and Guan [17] studied the dynamic interaction of a lined tunnel subjected to seismic loading in an infinite medium using the successive reflection method. More recently, Rembert et al. [18] applied the multichannel resonant scattering theory to study the wave interaction with an infinite fluid cylinder in an elastic medium. Rhee and Park [19] also presented a new method to analyze the elastic wave resonance scattering from a water-filled cylindrical cavity embedded in an aluminum matrix. Robert et al. [20] studied the scattering of elastic wave by a cylindrical cavity embedded in an elastic medium.

The preceding review has primarily focused on the research work involving cavities or tunnels in a single-phase elastic medium. However, many geotechnical engineering applications require multi-phase model of the soil. In fact, the growing body of literature suggested that under certain conditions there are significant differences in modeling the soil as a saturated poroelastic medium rather than a single-phase elastic medium. For the saturated porous media, several scholars have also addressed the scattering of elastic wave by an embedded cavity. Mei et al. [21] used the boundary layer approximation to study the scattering by a cylindrical cavity in a boundless porous solid. Krutin et al. [22] solved the problem of elastic harmonic wave by a fluid-filled cylindrical cavity embedded in a saturated medium. Zimmerman [23] used the boundary element method to study the problem of wave diffraction by a spherical cavity in an infinite poroelastic medium. Senjuntichat and Rajapakse [24] employed Biot's equations for poroelastodynamics in combination with the Laplace transform technique to investigate the transient response of a long cylindrical cavity in an infinite poroelastic medium. Hu et al. [25] studied the scattering and refraction of plane strain wave by a cylindrical cavity in a saturated medium. Lin et al. [26] investigated the effect of stiffness and Possion's ratio for *P* and *SV* wave reflected by a free surface of a poroelastic half-space. Kattis et al. [27] investigated the two-dimensional dynamic response of the unlined and lined tunnel in a porous soil due to harmonic wave. Gatmiri and Eslami [28] presented the complex function approach to analyze the scattering of harmonic wave by a circular cavity in an infinite poroelastic medium. Lu and Wang [29] used the complex variable method to solve the problem of the scattering of elastic wave by cavity of arbitrary shape in a saturated soil. Wang et al. [30] used the potential function and the complex function method to solve the scattering of plane wave by multiple elliptic cavities in a saturated medium. Lu et al. [31] investigated the frequency domain response of a circular tunnel with prefabricated piecewise lining subjected to seismic wave using the wave function expansion method. Hasheminejad and Avazmohammadi [32] studied the dynamic interaction of a pair of parallel cylindrical cavities embedded in a boundless porous saturated medium due to incident plane wave.

The above review indicates that a relative large body of literature on the elastic wave scattering by cavities or tunnels embedded in a single-phase elastic medium is studied, but the analytic or numerical solutions involving multiple lined tunnels in a poroelastic medium seem to be nonexistent. Our purpose of the present study is to develop a semi-analytical method for addressing the scattering of elastic wave by a pair of elliptic lined tunnels in a poroelastic medium. The attention has been focused on the multiple scattering and the interaction effect between two tunnels. The poroelastic medium is described by Biot's theory [33,34]. By introducing three potentials, the governing equations for Biot's theory are decoupled and reduced to three Helmholtz equations. The lined tunnel is treated as a single-phase elastic medium. The two regions are coupled through the continuation conditions at the interface of the poroelastic medium and tunnels. To illustrate the result of this solution, the dimensionless wavenumber, elliptic ratio, distance between two tunnels and thickness of liner influence on the dynamic stresses and the pore pressures around tunnels are studied.

2. Governing equations for poroelastic medium

In this study, the two elliptic lined tunnels are considered to be infinitely long, while the incident plane wave has a direction perpendicular to the axis of the tunnels. Thus, the dynamic interaction between two tunnels and its surrounding medium can be reduced to a plane strain problem (Fig. 1). The surrounding medium of the tunnels is considered as a saturated porous medium and described by Biot's theory [33,34].

2.1. Biot's theory

Based on Biot's theory, the constitutive equations for a homogeneous poroelastic medium are expressed as [33,34]

$$\sigma_{ij} = 2\mu\varepsilon_{ij} + \lambda\delta_{ij}e - \alpha\delta_{ij}p_f \tag{1}$$

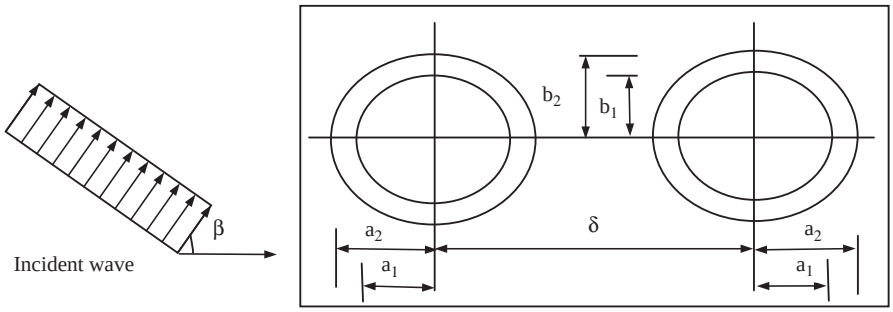

Fig. 1. Incident wave by a pair of elliptic lined tunnels in a poroelastic medium.

$$p_f = -\alpha M e + M\vartheta \tag{2}$$

$$e = u_{i,i}, \quad \vartheta = -w_{i,i} \tag{3}$$

where σ_{ij} is the stress of the bulk material; ε_{ij} and e are the strain tensor and the dilatation of the solid skeleton, respectively; λ and μ are Lamé constants; δ_{ij} is the Kronecker delta; ϑ is the volume of fluid injection into unit volume of the bulk material; α and M are Biot parameters; p_f is the excess pore pressure; u_i and w_i denote the average solid displacement and the infiltration displacement of the pore fluid.

The equations of motion for the poroelastic medium can be expressed in terms of the displacements u_i and w_i

$$\mu u_{i,jj} + (\lambda + \alpha^2 M + \mu) u_{j,ji} + \alpha M w_{j,ji} = \rho \ddot{u}_i + \rho_f \ddot{w}_i \tag{4}$$

$$\alpha M u_{j,ji} + M w_{j,ji} = \rho_f \ddot{u}_i + \frac{\rho_f}{n} \ddot{w}_i + \frac{\eta}{k} \dot{w}_i \tag{5}$$

where ρ and ρ_f denote the bulk density of the porous medium and the density of the pore fluid, respectively; $\rho = (1-n)\rho_s + n\rho_f$, ρ_s is the density of the solid skeleton and n is the porosity of the porous medium; k and η represent the permeability and the fluid viscosity, respectively; a superimposed dot denotes the derivative with respect to time t.

In order to eliminate time derivatives in Eqs. (4)–(5), the Fourier transformation with respect to time t is performed on Eqs. (1)–(5). As a result, all the governing equations are transformed into the frequency domain. Accordingly, the following derivations will be developed in the frequency domain.

To derive the general solutions for Biot's equations, two scalar potentials φ_f, φ_s and one vector potential ψ are introduced to express the displacement and the pore pressure of the porous medium. The displacement and the pore pressure are expressed by the potentials in the following form [31]:

$$\hat{u}_i = \hat{\varphi}_{,i} + e_{ijk}\hat{\psi}_{k,j} = \hat{\varphi}_{f,i} + \hat{\varphi}_{s,i} + e_{ijk}\hat{\psi}_{k,j} \tag{6}$$

$$\hat{p}_f = A_f \hat{\varphi}_{f,ii} + A_s \hat{\varphi}_{s,ii} \tag{7}$$

where a caret denotes the Fourier transform with respect to time; e_{ijk} is the Levi–Civita symbol; $\hat{\varphi}_f$, $\hat{\varphi}_s$ denote the scalar potentials corresponding to P_1 wave and P_2 wave, respectively; A_f and A_s are two constants to be determined by the governing equations of Biot's theory.

Using the frequency domain expressions of Eq. (2) and Eqs. (4)–(5) as well as Eqs. (6)–(7) leads to [29,30]

$$[(\lambda + 2\mu - \beta_2 A_f)\hat{\varphi}_{f,jj} + \beta_3 \hat{\varphi}_f]_{,i} + [(\lambda + 2\mu - \beta_2 A_s)\hat{\varphi}_{s,jj} + \beta_3 \hat{\varphi}_s]_{,i} + e_{iml}[\mu \hat{\psi}_{i,jj} + \beta_3 \hat{\psi}_i]_{,m} = 0 \tag{8}$$

Fulfillment of the above equation requires that the expressions in braces vanish independently, which gives the following equations for the potentials:

$$(\lambda + 2\mu - \beta_2 A_f)\hat{\varphi}_{f,jj} + \beta_3 \hat{\varphi}_f = 0 \tag{9}$$

$$(\lambda + 2\mu - \beta_2 A_s)\hat{\varphi}_{s,jj} + \beta_3 \hat{\varphi}_s = 0 \tag{10}$$

$$\mu \hat{\psi}_{i,jj} + \beta_3 \hat{\psi}_i = 0 \tag{11}$$

where $\beta_3 = \rho\omega^2 + \rho_f^2\omega^4/\beta_1$; $\beta_2 = \alpha + \rho_f\omega^2/\beta_1$; $\beta_1 = -\rho_f\omega^2/n - \mathrm{i}\eta\omega/k$ and ω is the frequency.

Substituting of Eqs. (2)–(3) into Eq. (5) yields

$$\hat{p}_{f,ii} - \frac{\beta_1}{M}\hat{p}_f - (\alpha\beta_1 + \rho_f\omega^2)\hat{u}_{i,i} = 0 \tag{12}$$

Likewise, substituting Eqs. (6)–(7) into the above equation yields

$$[A_f\hat{\varphi}_{f,ii}+(\beta_5A_f-\beta_4)\hat{\varphi}_f]_{,jj}+[A_s\hat{\varphi}_{s,ii}+(\beta_5A_s-\beta_4)\hat{\varphi}_s]_{,jj}=0 \tag{13}$$

The following equations can be derived from Eq. (13)

$$A_f\hat{\varphi}_{f,ii}+(\beta_5A_f-\beta_4)\hat{\varphi}_f=0 \tag{14}$$

$$A_s\hat{\varphi}_{s,ii}+(\beta_5A_s-\beta_4)\hat{\varphi}_s=0 \tag{15}$$

where $\beta_4=\alpha\beta_1+\rho_f\omega^2$; $\beta_5=-\beta_1/M$. In terms of Eqs. (9)–(10) and (14)–(15), the following equation determining A_f and A_s is obtained

$$A_{f,s}^2+\frac{\beta_3-(\lambda+2\mu)\beta_5-\beta_2\beta_4}{\beta_2\beta_5}A_{f,s}+\frac{(\lambda+2\mu)\beta_4}{\beta_2\beta_5}=0 \tag{16}$$

It should be noted that the values of A_f and A_s can be determined by Eq. (16), if the following quantities are introduced.

$$k_f^2=\beta_3/(\lambda+2\mu-\beta_2A_f)=(\beta_5A_f-\beta_4)/A_f \tag{17}$$

$$k_s^2=\beta_3/(\lambda+2\mu-\beta_2A_s)=(\beta_5A_s-\beta_4)/A_s \tag{18}$$

$$k_t^2=\beta_3/\mu \tag{19}$$

where k_f, k_s and k_t are the complex wavenumbers for P_1, P_2 and S wave of the porous medium. Since the speed of the P_1 wave is faster than that of the P_2 wave, as a result, the inequality $\mathrm{Re}(k_f)\leqslant\mathrm{Re}(k_s)$ should also hold.

Then, Eqs. (9)–(11) can be reduced to the following Helmholtz equations:

$$\nabla^2\hat{\varphi}_f+k_f^2\hat{\varphi}_f=0 \tag{20}$$

$$\nabla^2\hat{\varphi}_s+k_s^2\hat{\varphi}_s=0 \tag{21}$$

$$\nabla^2\hat{\psi}+k_k^2\hat{\psi}=0 \tag{22}$$

As mentioned previously, the proposed problem can be treated as a plane strain problem. For the plane strain problem, u_3 and w_3 should vanish, consequently, the vector potential $\hat{\psi}$ in Eq. (22) has only one component, i.e. $\hat{\psi}_3$. For simplicity, $\hat{\psi}_3$ is written as $\hat{\psi}$ in what follows. Obviously, $\hat{\psi}$ satisfies the following Helmholtz equation.

$$\nabla^2\hat{\psi}+k_t^2\hat{\psi}=0 \tag{23}$$

2.2. Expressions of displacements, stresses and pore pressures

For plane strain problem of a poroelastic medium, the displacement of the solid skeleton, the stress and the pore pressure can be represented by three potentials $\hat{\varphi}_f$, $\hat{\varphi}_s$ and $\hat{\psi}$. When introducing complex variables $z=x+\mathrm{i}y$, $\bar{z}=x-\mathrm{i}y$, one can obtain the following displacement and stress combinations:

$$\hat{u}_{\tilde{x}_I}+\mathrm{i}\hat{u}_{\tilde{y}_I}=2\frac{\partial}{\partial\bar{z}}(\hat{\varphi}_f+\hat{\varphi}_s-\mathrm{i}\hat{\psi})\mathrm{e}^{-\mathrm{i}\gamma} \tag{24}$$

$$\hat{u}_{\tilde{x}_I}-\mathrm{i}\hat{u}_{\tilde{y}_I}=2\frac{\partial}{\partial z}(\hat{\varphi}_f+\hat{\varphi}_s+\mathrm{i}\hat{\psi})\mathrm{e}^{\mathrm{i}\gamma} \tag{25}$$

$$\hat{w}_{\tilde{x}_I}=\frac{\partial}{\partial z}(\eta_1\hat{\varphi}_f+\eta_2\hat{\varphi}_s+\mathrm{i}\alpha_1\hat{\psi})\mathrm{e}^{\mathrm{i}\gamma}+\frac{\partial}{\partial\bar{z}}(\eta_1\hat{\varphi}_f+\eta_2\hat{\varphi}_s-\mathrm{i}\alpha_1\hat{\psi})\mathrm{e}^{-\mathrm{i}\gamma} \tag{26}$$

$$\hat{\sigma}_{\tilde{x}_1}-\mathrm{i}\hat{\sigma}_{x\tilde{y}_1}=\alpha_f\hat{\varphi}_f+\alpha_s\hat{\varphi}_s+4\mu_l\frac{\partial^2}{\partial z^2}(\hat{\varphi}_f+\hat{\varphi}_s+\mathrm{i}\hat{\psi})\mathrm{e}^{2\mathrm{i}\gamma} \tag{27}$$

$$\hat{\sigma}_{\tilde{x}_I}+\mathrm{i}\hat{\sigma}_{x\tilde{y}_I}=\alpha_f\hat{\varphi}_f+\alpha_s\hat{\varphi}_s+4\mu_l\frac{\partial^2}{\partial\bar{z}^2}(\hat{\varphi}_f+\hat{\varphi}_s-\mathrm{i}\hat{\psi})\mathrm{e}^{-2\mathrm{i}\gamma} \tag{28}$$

$$\hat{p}_{f_1}=-A_fk_f^2\hat{\varphi}_f-A_sk_s^2\hat{\varphi}_s \tag{29}$$

where $\alpha_f=\alpha A_fk_f^2-(\lambda+\mu_l)k_f^2$; $\alpha_s=\alpha A_sk_s^2-(\lambda+\mu_l)k_s^2$; $\eta_1=\alpha_1-\alpha_2A_fk_f^2$; $\eta_2=\alpha_1-\alpha_2A_sk_s^2$; $\alpha_1=\rho_f\omega^2/\beta_1$; $\alpha_2=-1/\beta_1$, and subscript I designates the functions in the poroelastic medium; superscript $\sim$ denotes the functions in the coordinate transform.

Note that the displacement and stress combinations in above equations are in the coordinate system $\tilde{x}o\tilde{y}$ in the z plane, which is obtained rotating the coordinate system xoy by an angle γ. Also, the expression for the pore pressure Eq. (29) does not vary when performing coordinate rotation.

We selected elliptic tunnel as example, the equation of the j-th elliptic tunnel can be expressed as:

$$f(x_j, y_j) = \frac{x_j^2}{a_j^2} + \frac{y_j^2}{b_j^2} - 1 = 0 \tag{30}$$

where a_j and b_j are the long axial radius and the short axial radius, respectively.

On the boundary of the j-th elliptic tunnel

$$x_j = r_j \cos\theta, \quad y_j = r_j \sin\theta \tag{31}$$

$$r_j = \frac{a_j}{\sqrt{\cos^2\theta + \frac{a_j^2}{b_j^2}\sin^2\theta}} \tag{32}$$

$$\gamma_j = tg^{-1}\left(\frac{a_j^2}{b_j^2} tg\theta\right) \tag{33}$$

2.3. The incident wave and the scattered wave

Due to the presence of the two elliptic tunnels (Fig. 1), the total wave in the poroelastic medium in presence of the tunnels consists of two parts: the incident wave field and the scattered wave field. The total wave field can be expressed as:

$$\varphi_f = \varphi_f^{(I)} + \sum_{j=1}^{2} \varphi_{fj}^{(S)} = \varphi_f^{(I)} + \varphi_f^{(S)}, \quad \varphi_s = \varphi_s^{(I)} + \sum_{j=1}^{2} \varphi_{sj}^{(S)} = \varphi_s^{(I)} + \varphi_s^{(S)}, \quad \psi = \psi^{(I)} + \sum_{j=1}^{2} \psi_j^{(S)} = \psi^{(I)} + \psi^{(S)} \tag{34}$$

where superscript I denotes the incident wave; superscript S denotes the scattered wave.

Since the potential for the incident wave field satisfies the Helmholtz equations, accordingly, the potential for the scattered field should also satisfy the corresponding Helmholtz equations. Therefore, the general solutions of Eqs. (20)–(22) may be expressed in terms of Hankel functions as:

$$\varphi_{fj}^{(S)} = \sum_{n=-\infty}^{\infty} a_{jn} H_n^{(1)}(k_f|z_j|)\left(\frac{z_j}{|z_j|}\right)^n \tag{35}$$

$$\varphi_{sj}^{(S)} = \sum_{n=-\infty}^{\infty} b_{jn} H_n^{(1)}(k_s|z_j|)\left(\frac{z_j}{|z_j|}\right)^n \tag{36}$$

$$\psi_j^{(S)} = \sum_{n=-\infty}^{\infty} c_{jn} H_n^{(1)}(k_t|z_j|)\left(\frac{z_j}{|z_j|}\right)^n \tag{37}$$

where $H_n^{(1)}(*)$ is the first kind of Hankel function; a_{jn}, b_{jn}, c_{jn} are arbitrary functions to be determined from the boundary conditions of the j-th tunnels ($j = 1,2$).

The total scattered waves can also be expressed as:

$$\varphi_f^{(S)} = \sum_{j=1}^{2}\sum_{n=-\infty}^{\infty} a_{jn} H_n^{(1)}(k_f|z-d_j|)\left(\frac{z-d_j}{|z-d_j|}\right)^n \tag{38}$$

$$\varphi_s^{(S)} = \sum_{j=1}^{2}\sum_{n=-\infty}^{\infty} b_{jn} H_n^{(1)}(k_s|z-d_j|)\left(\frac{z-d_j}{|z-d_j|}\right)^n \tag{39}$$

$$\psi^{(S)} = \sum_{j=1}^{2}\sum_{n=-\infty}^{\infty} c_{jn} H_n^{(1)}(k_t|z-d_j|)\left(\frac{z-d_j}{|z-d_j|}\right)^n \tag{40}$$

where d_j is the distance between the origin of j-th tunnel and the origin of total coordinate system.

3. Governing equations for the liners

In this study, as the interaction between the tunnels and its surrounding poroelastic medium is treated as a plane strain problem, and the equation for liner can be expressed as

$$\mu u_{i,jj} + (\lambda + \mu) u_{j,ji} = \rho \ddot{u}_i \tag{41}$$

where ρ denotes the density of the liner; λ, μ represent Lamé constants of the liner.

There are four refracted wave in the j-th liner: two inward propagating waves and two outward propagating waves excited by the incident plane wave.

$$\varphi_j^{(F)} = \sum_{n=-\infty}^{\infty} (d_{jn} H_n^{(1)}(k_p|z_j|) + e_{jn} H_n^{(2)}(k_p|z_j|)) \left(\frac{z_j}{|z_j|}\right)^n \tag{42}$$

$$\psi_j^{(F)} = \sum_{n=-\infty}^{\infty} (m_{jn} H_n^{(1)}(k_s|z_j|) + n_{jn} H_n^{(2)}(k_s|z_j|)) \left(\frac{z_j}{|z_j|}\right)^n \tag{43}$$

where superscript F denotes the refracted wave; $H_n^{(2)}(*)$ denotes the second kind of Hankel function; $k_p^2 = \omega^2/V_p^2$; $V_p = \sqrt{(\lambda + 2\mu)/\rho}$; $k_s^2 = \omega^2/V_s^2$; $V_s = \sqrt{\mu/\rho}$; k_p, k_s denote the complex wavenumbers for the compressional wave and the shear wave; d_{jn}, e_{jn}, m_{jn}, n_{jn} are arbitrary functions to be determined from the boundary conditions of the j-th tunnel ($j = 1, 2$).

When rotating the coordinate system xoy by an angle γ and introducing complex variables $z = x + \mathrm{i}y$, $\bar{z} = x - \mathrm{i}y$, the displacement and the stress of liner have the following expressions:

$$\hat{u}_{\tilde{x}_{II}} + \mathrm{i}\hat{u}_{\tilde{y}_{II}} = 2\frac{\partial}{\partial \bar{z}}(\hat{\varphi} - \mathrm{i}\hat{\psi})\mathrm{e}^{-\mathrm{i}\gamma} \tag{44}$$

$$\hat{u}_{\tilde{x}_{II}} - \mathrm{i}\hat{u}_{\tilde{y}_{II}} = 2\frac{\partial}{\partial z}(\hat{\varphi} + \mathrm{i}\hat{\psi})\mathrm{e}^{\mathrm{i}\gamma} \tag{45}$$

$$\hat{\sigma}_{\tilde{x}_{II}} - \mathrm{i}\hat{\sigma}_{x\tilde{y}_{II}} = 4\mu_{II}\frac{\partial^2}{\partial z^2}(\hat{\varphi} + \mathrm{i}\hat{\psi})\mathrm{e}^{2\mathrm{i}\gamma} \tag{46}$$

$$\hat{\sigma}_{\tilde{x}_{II}} + \mathrm{i}\hat{\sigma}_{x\tilde{y}_{II}} = 4\mu_{II}\frac{\partial^2}{\partial \bar{z}^2}(\hat{\varphi} - \mathrm{i}\hat{\psi})\mathrm{e}^{-2\mathrm{i}\gamma} \tag{47}$$

where subscript II designates functions in liner.

4. Formulation of the boundary value problems

The surrounding poroelastic medium and the tunnels are treated separately in the above sections. When subjected to seismic wave, the stresses and the displacements should be continuous at the boundary between the tunnels and the poroelastic medium. At the conjunctive surface of the poroelastic medium and the tunnels, the continuation conditions between the poroelastic medium and the tunnels are as follows

$$\hat{u}_{\tilde{x}_I} + \mathrm{i}\hat{u}_{\tilde{y}_I} = \hat{u}_{\tilde{x}_{II}} + \mathrm{i}\hat{u}_{\tilde{y}_{II}} \tag{48}$$

$$\hat{u}_{\tilde{x}_I} - \mathrm{i}\hat{u}_{\tilde{y}_I} = \hat{u}_{\tilde{x}_{II}} - \mathrm{i}\hat{u}_{\tilde{y}_{II}} \tag{49}$$

$$\hat{\sigma}_{\tilde{x}_I} - \mathrm{i}\hat{\sigma}_{x\tilde{y}_I} = \hat{\sigma}_{\tilde{x}_{II}} - \mathrm{i}\hat{\sigma}_{x\tilde{y}_{II}} \tag{50}$$

$$\hat{\sigma}_{\tilde{x}_I} + \mathrm{i}\hat{\sigma}_{x\tilde{y}_I} = \hat{\sigma}_{\tilde{x}_{II}} + \mathrm{i}\hat{\sigma}_{x\tilde{y}_{II}} \tag{51}$$

For impermeable boundary condition, the displacement of the fluid relative to the solid skeleton should vanish. Therefore, Eq. (26) obtains

$$\hat{w}_{\tilde{x}_1} = 0 \tag{52}$$

At inner surface of the liner, the stress free conditions are

$$\hat{\sigma}_{\tilde{x}_{II}} - \mathrm{i}\hat{\sigma}_{x\tilde{y}_{II}} = 0 \tag{53}$$

$$\hat{\sigma}_{\tilde{x}_{II}} + \mathrm{i}\hat{\sigma}_{x\tilde{y}_{II}} = 0 \tag{54}$$

Substituting of Eqs. (24)–(25), (44)–(45) into Eqs. (48)–(49), using Eqs. (34)–(37) and (42)–(43), one obtains

$$\sum_{p=1}^{7}\sum_{i=1}^{2}\sum_{n=-\infty}^{\infty} E^1_{kpin}x_{pin} = r^1_{kj} \quad (k,j=1,2) \tag{55}$$

where

$$E^1_{11in} = -k_f H^{(1)}_{n+1}(k_f|\xi_{ij}|)\left(\frac{\xi_{ij}}{|\xi_{ij}|}\right)^{n+1} \mathrm{e}^{-\mathrm{i}r_j} \tag{56a}$$

$$E^1_{12in} = -k_s H^{(1)}_{n+1}(k_s|\xi_{ij}|)\left(\frac{\xi_{ij}}{|\xi_{ij}|}\right)^{n+1} \mathrm{e}^{-\mathrm{i}r_j} \tag{56b}$$

$$E^1_{13in} = \mathrm{i}k_t H^{(1)}_{n+1}(k_t|\xi_{ij}|)\left(\frac{\xi_{ij}}{|\xi_{ij}|}\right)^{n+1} \mathrm{e}^{-\mathrm{i}r_j} \tag{56c}$$

$$E^1_{14in} = k_p H^{(1)}_{n+1}(k_p|\xi_{ij}|)\left(\frac{\xi_{ij}}{|\xi_{ij}|}\right)^{n+1} \mathrm{e}^{-\mathrm{i}r_j} \tag{56d}$$

$$E^1_{15in} = k_p H^{(2)}_{n+1}(k_p|\xi_{ij}|)\left(\frac{\xi_{ij}}{|\xi_{ij}|}\right)^{n+1} \mathrm{e}^{-\mathrm{i}r_j} \tag{56e}$$

$$E^1_{16in} = -\mathrm{i}k_s H^{(1)}_{n+1}(k_s|\xi_{ij}|)\left(\frac{\xi_{ij}}{|\xi_{ij}}\right)^{n+1} \mathrm{e}^{-\mathrm{i}r_j} \tag{56f}$$

$$E^1_{17in} = -\mathrm{i}k_s H^{(2)}_{n+1}(k_s|\xi_{ij}|)\left(\frac{\xi_{ij}}{|\xi_{ij}|}\right)^{n+1} \mathrm{e}^{-\mathrm{i}r_j} \tag{56g}$$

$$E^1_{21in} = k_f H^{(1)}_{n-1}(k_f|\xi_{ij}|)\left(\frac{\xi_{ij}}{|\xi_{ij}|}\right)^{n-1} \mathrm{e}^{\mathrm{i}r_j} \tag{56h}$$

$$E^1_{22in} = k_s H^{(1)}_{n-1}(k_s|\xi_{ij}|)\left(\frac{\xi_{ij}}{|\xi_{ij}|}\right)^{n-1} \mathrm{e}^{\mathrm{i}r_j} \tag{56i}$$

$$E^1_{23in} = \mathrm{i}k_t H^{(1)}_{n-1}(k_t|\xi_{ij}|)\left(\frac{\xi_{ij}}{|\xi_{ij}|}\right)^{n-1} \mathrm{e}^{\mathrm{i}r_j} \tag{56j}$$

$$E^1_{24in} = -k_p H^{(1)}_{n-1}(k_p|\xi_{ij}|)\left(\frac{\xi_{ij}}{|\xi_{ij}|}\right)^{n-1} \mathrm{e}^{\mathrm{i}r_j} \tag{56k}$$

$$E^1_{25in} = -k_p H^{(2)}_{n-1}(k_p|\xi_{ij}|)\left(\frac{\xi_{ij}}{|\xi_{ij}|}\right)^{n-1} \mathrm{e}^{\mathrm{i}r_j} \tag{56l}$$

$$E^1_{26in} = -\mathrm{i}k_s H^{(1)}_{n-1}(k_s|\xi_{ij}|)\left(\frac{\xi_{ij}}{|\xi_{ij}|}\right)^{n-1} \mathrm{e}^{\mathrm{i}r_j} \tag{56m}$$

$$E^1_{27in} = -\mathrm{i}k_s H^{(2)}_{n-1}(k_s|\xi_{ij})\left(\frac{\xi_{ij}}{|\xi_{ij}}\right)^{n-1} \mathrm{e}^{\mathrm{i}r_j} \tag{56n}$$

$$r^1_{1j} = -2\frac{\partial}{\partial \bar{z}_j}(\varphi^{(I)}_{fI} + \varphi^{(I)}_{sI} - \mathrm{i}\psi^{(I)}_I)\mathrm{e}^{-\mathrm{i}\gamma_j} \tag{57a}$$

$$r^1_{2j} = -2\frac{\partial}{\partial z_j}(\varphi^{(I)}_{fI} + \varphi^{(I)}_{sI} + \mathrm{i}\psi^{(I)}_I)\mathrm{e}^{\mathrm{i}\gamma_j} \tag{57b}$$

$$x_{1in}=a_{in},\quad x_{2in}=b_{in},\quad x_{3in}=c_{in},\quad x_{4in}=d_{in},\quad x_{5in}=e_{in},\quad x_{6in}=m_{in},\quad x_{7in}=n_{in} \tag{58}$$

where $\xi_{ij}=z_j e^{i\alpha_j}+d_j-d_i$; $z_j=r_j e^{i\theta}$.

Multiplying both sides of Eq. (55) with $e^{-is\theta}$ and integrating over the interval $[-\pi,\pi]$ yields

$$\sum_{p=1}^{7}\sum_{i=1}^{2}\sum_{n=-\infty}^{n=\infty}E^{1s}_{kpin}x_{pin}=r^{1s}_{kj}\quad(k,j=1,2)\quad(s=0,\pm1,\pm2,\ldots) \tag{59}$$

where

$$E^{1s}_{kpin}=\frac{1}{2\pi}\int_{-\pi}^{\pi}E^{1}_{kpin}e^{-is\theta}\,d\theta\quad(s=0,\pm1,\pm2,\ldots) \tag{60a}$$

$$r^{1s}_{kj}=\frac{1}{2\pi}\int_{-\pi}^{\pi}r^{1}_{kj}e^{-is\theta}\,d\theta\quad(s=0,\pm1,\pm2,\ldots) \tag{60b}$$

Likewise, substituting of Eqs. (26)–(27), (46)–(47) into Eqs. (50) and (51) , using Eqs. (34)–(37) and (42)–(43)

$$\sum_{p=1}^{7}\sum_{i=1}^{2}\sum_{n=-\infty}^{\infty}E^{2}_{kpin}x_{pin}=r^{2}_{kj}\quad(k,j=1,2) \tag{61}$$

where

$$E^{2}_{11in}=\alpha_f H^{(1)}_n(k_f|\zeta_{ij}|)\left(\frac{\zeta_{ij}}{|\zeta_{ij}|}\right)^n+\mu_I k_f^2 H^{(1)}_{n-2}(k_f|\zeta_{ij}|)\left(\frac{\zeta_{ij}}{|\zeta_{ij}|}\right)^{n-2}e^{2i\gamma_j} \tag{62a}$$

$$E^{2}_{12in}=\alpha_s H^{(1)}_n(k_s|\zeta_{ij}|)\left(\frac{\zeta_{ij}}{|\zeta_{ij}|}\right)^n+\mu_I k_s^2 H^{(1)}_{n-2}(k_s|\zeta_{ij}|)\left(\frac{\zeta_{ij}}{|\zeta_{ij}|}\right)^{n-2}e^{2i\gamma_j} \tag{62b}$$

$$E^{2}_{13in}=i\mu_I k_t^2 H^{(1)}_{n-2}(k_t|\zeta_{ij}|)\left(\frac{\zeta_{ij}}{|\zeta_{ij}|}\right)^{n-2}e^{2i\gamma_j} \tag{62c}$$

$$E^{2}_{14in}=-\mu_{II} k_p^2 H^{(1)}_{n-2}(k_p|\zeta_{ij}|)\left(\frac{\zeta_{ij}}{|\zeta_{ij}|}\right)^{n-2}e^{2i\gamma_j} \tag{62d}$$

$$E^{2}_{15in}=-\mu_{II} k_p^2 H^{(2)}_{n-2}(k_p|\zeta_{ij}|)\left(\frac{\zeta_{ij}}{|\zeta_{ij}|}\right)^{n-2}e^{2i\gamma_j} \tag{62e}$$

$$E^{2}_{16in}=-i\mu_{II} k_s^2 H^{(1)}_{n-2}(k_s|\zeta_{ij}|)\left(\frac{\zeta_{ij}}{|\zeta_{ij}|}\right)^{n-2}e^{2i\gamma_j} \tag{62f}$$

$$E^{2}_{17in}=-i\mu_{II} k_s^2 H^{(2)}_{n-2}(k_s|\zeta_{ij}|)\left(\frac{\zeta_{ij}}{|\zeta_{ij}|}\right)^{n-2}e^{2i\gamma_j} \tag{62g}$$

$$E^{2}_{21in}=\alpha_f H^{(1)}_n(k_f|\zeta_{ij}|)\left(\frac{\zeta_{ij}}{|\zeta_{ij}|}\right)^n+\mu_I k_f^2 H^{(1)}_{n+2}(k_f|\zeta_{ij}|)\left(\frac{\zeta_{ij}}{|\zeta_{ij}|}\right)^{n+2}e^{-2i\gamma_j} \tag{62h}$$

$$E^{2}_{22in}=\alpha_s H^{(1)}_n(k_s|\zeta_{ij}|)\left(\frac{\zeta_{ij}}{|\zeta_{ij}|}\right)^n+\mu_I k_s^2 H^{(1)}_{n+2}(k_s|\zeta_{ij}|)\left(\frac{\zeta_{ij}}{|\zeta_{ij}|}\right)^{n+2}e^{-2i\gamma_j} \tag{62i}$$

$$E^{2}_{23in}=-i\mu_I k_t^2 H^{(1)}_{n+2}(k_t|\zeta_{ij}|)\left(\frac{\zeta_{ij}}{|\zeta_{ij}|}\right)^{n+2}e^{-2i\gamma_j} \tag{62j}$$

$$E^{2}_{24in}=-\mu_{II} k_p^2 H^{(1)}_{n+2}(k_p|\zeta_{ij}|)\left(\frac{\zeta_{ij}}{|\zeta_{ij}|}\right)^{n+2}e^{-2i\gamma_j} \tag{62k}$$

$$E^2_{25in} = -\mu_{II}k_p^2 H^{(2)}_{n+2}(k_p|\zeta_{ij}|)\left(\frac{\zeta_{ij}}{|\zeta_{ij}|}\right)^{n+2} e^{-2i\gamma_j} \tag{62l}$$

$$E^2_{26in} = i\mu_{II}k_s^2 H^{(1)}_{n+2}(k_s|\zeta_{ij}|)\left(\frac{\zeta_{ij}}{|\zeta_{ij}|}\right)^{n+2} e^{-2i\gamma_j} \tag{62m}$$

$$E^2_{27in} = i\mu_{II}k_s^2 H^{(2)}_{n+2}(k_s|\zeta_{ij}|)\left(\frac{\zeta_{ij}}{|\zeta_{ij}|}\right)^{n+2} e^{-2i\gamma_j} \tag{62n}$$

$$r^2_{1j} = -\alpha_f\varphi_f^{(I)} - \alpha_s\varphi_s^{(I)} - \mu_I\frac{\partial^2}{\partial z_j^2}(\varphi_{fI}^{(I)} + \varphi_{sI}^{(I)} + i\hat{\psi}_I^{(I)})e^{2i\gamma_j} \tag{63a}$$

$$r^2_{2j} = -\alpha_f\varphi_f^{(I)} - \alpha_s\varphi_s^{(I)} - \mu_I\frac{\partial^2}{\partial \bar{z}_j^2}(\varphi_{fI}^{(I)} + \varphi_{sI}^{(I)} - i\hat{\psi}_I^{(I)})e^{-2i\gamma_j} \tag{63b}$$

Multiplying both sides of Eq. (61) with $e^{-is\theta}$, and integrating over the interval $[-\pi, \pi]$ yields

$$\sum_{p=1}^{7}\sum_{i=1}^{2}\sum_{n=-\infty}^{n=\infty} E^{2s}_{kpin}x_{pin} = r^{2s}_{kj} \quad (k,j=1,2) \quad (s=0,\pm1,\pm2,\ldots) \tag{64}$$

where

$$E^{2s}_{kpin} = \frac{1}{2\pi}\int_{-\pi}^{\pi} E^2_{kpin}e^{-is\theta}\,d\theta \quad (s=0,\pm1,\pm2,\ldots) \tag{65a}$$

$$r^{2s}_{kj} = \frac{1}{2\pi}\int_{-\pi}^{\pi} r^2_{kj}e^{-is\theta}\,d\theta \quad (s=0,\pm1,\pm2,\ldots) \tag{65b}$$

For impermeable boundary condition, the normal displacement of the fluid to the solid skeleton of the j-th cavities should vanish. Eq. (52) gives

$$\sum_{p=1}^{3}\sum_{i=1}^{2}\sum_{n=-\infty}^{\infty} E^3_{pin}x_{pin} = r^3_j \quad (j=1,2) \tag{66}$$

where

$$E^3_{1in} = \frac{\eta_1 k_f}{2}H^{(1)}_{n-1}(k_f|\zeta_{ij}|)\left(\frac{\zeta_{ij}}{|\zeta_{ij}|}\right)^{n-1} e^{i\gamma_j} - \frac{\eta_1 k_f}{2}H^{(1)}_{n+1}(k_f|\zeta_{ij}|)\left(\frac{\zeta_{ij}}{|\zeta_{ij}|}\right)^{n+1} e^{-i\gamma_j} \tag{67a}$$

$$E^3_{2in} = \frac{\eta_2 k_s}{2}H^{(1)}_{n-1}(k_s|\zeta_{ij}|)\left(\frac{\zeta_{ij}}{|\zeta_{ij}|}\right)^{n-1} e^{i\gamma_j} - \frac{\eta_2 k_s}{2}H^{(1)}_{n+1}(k_s|\zeta_{ij}|)\left(\frac{\zeta_{ij}}{|\zeta_{ij}|}\right)^{n+1} e^{-i\gamma_j} \tag{67b}$$

$$E^3_{3in} = \frac{i\alpha_1 k_t}{2}H^{(1)}_{n-1}(k_t|\zeta_{ij}|)\left(\frac{\zeta_{ij}}{|\zeta_{ij}|}\right)^{n-1} e^{i\gamma_j} + \frac{i\alpha_1 k_t}{2}H^{(1)}_{n+1}(k_t|\zeta_{ij}|)\left(\frac{\zeta_{ij}}{|\zeta_{ij}|}\right)^{n+1} e^{-i\gamma_j} \tag{67c}$$

Table 1
Input parameter values used in porous medium and liner.

Parameter	Porous medium	Parameter	Liner
ρ_s (kg/m^3)	2000	ρ (kg/m^3)	3000
ρ_f (kg/m^3)	1000	v	0.35
n	0.25	μ (Pa)	3.0×10^5
μ (Pa)	1.0×10^7		
v	0.25		
α	0.999		
M (Pa)	1.0×10^8		
η (Pa)	1.0×10^{-2}		
k' (m^2)	1.0×10^{-7}		

$$r_j^3 = -\frac{\partial}{\partial z_j}(\eta_1\varphi_f^{(l)} + \eta_2\varphi_s^{(l)} + \alpha_1 i\hat{\psi}^{(l)})e^{i\gamma_j} - \frac{\partial}{\partial \bar{z}_j}(\eta_1\varphi_f^{(l)} + \eta_2\varphi_s^{(l)} - \alpha_1 i\hat{\psi}^{(l)})e^{-i\gamma_j} \tag{68}$$

Multiplying both sides of Eq. (66) with $e^{-is\theta}$, and integrating over the interval $[-\pi, \pi]$ yields

$$\sum_{p=1}^{3}\sum_{i=1}^{2}\sum_{n=-\infty}^{\infty} E_{pin}^{3s} x_{pin} = r_j^{3s} \quad (j = 1, 2) \quad (s = 0, \pm 1, \pm 2, \ldots) \tag{69}$$

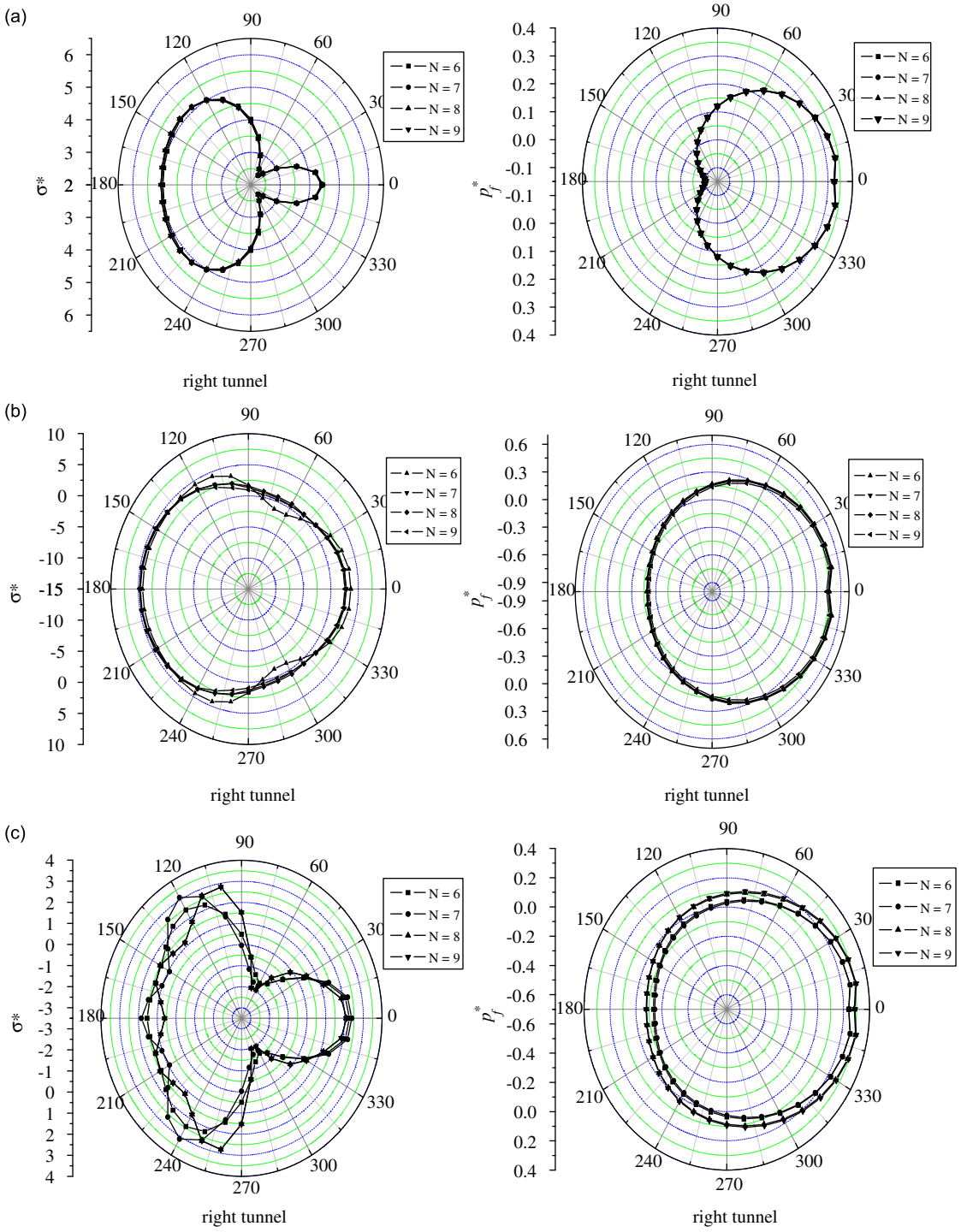

Fig. 2. A convergence test for two lined tunnels: (a) $\mathrm{Re}(k_f a) = 0.1$; (b) $\mathrm{Re}(k_f a) = 0.2$; and (c) $\mathrm{Re}(k_f a) = 0.3$.

where

$$E^{3s}_{pin} = \frac{1}{2\pi}\int_{-\pi}^{\pi} E^{3}_{pin} e^{-is\theta}\, d\theta \quad (s = 0, \pm 1, \pm 2, \ldots) \tag{70a}$$

$$r^{3s}_{j} = \frac{1}{2\pi}\int_{-\pi}^{\pi} r^{3}_{j} e^{-is\theta}\, d\theta \quad (s = 0, \pm 1, \pm 2, \ldots) \tag{70b}$$

Substituting of Eqs. (46) and (47) into Eqs. (53) and (54), using Eqs. (34)–(37) and (42) (43)

$$\sum_{p=1}^{4}\sum_{i=1}^{2}\sum_{n=-\infty}^{\infty} E^{4}_{kpin} x_{pin} = r^{4}_{kj} \quad (k,j = 1,2) \tag{71}$$

where

$$E^{4}_{11in} = \mu_{II} k_p^2 H^{(1)}_{n-2}(k_p|\zeta_{ij}|)\left(\frac{\zeta_{ij}}{|\zeta_{ij}|}\right)^{n-2} e^{2i\gamma_j} \tag{72a}$$

$$E^{4}_{12in} = \mu_{II} k_p^2 H^{(2)}_{n-2}(k_p|\zeta_{ij}|)\left(\frac{\zeta_{ij}}{|\zeta_{ij}|}\right)^{n-2} e^{2i\gamma_j} \tag{72b}$$

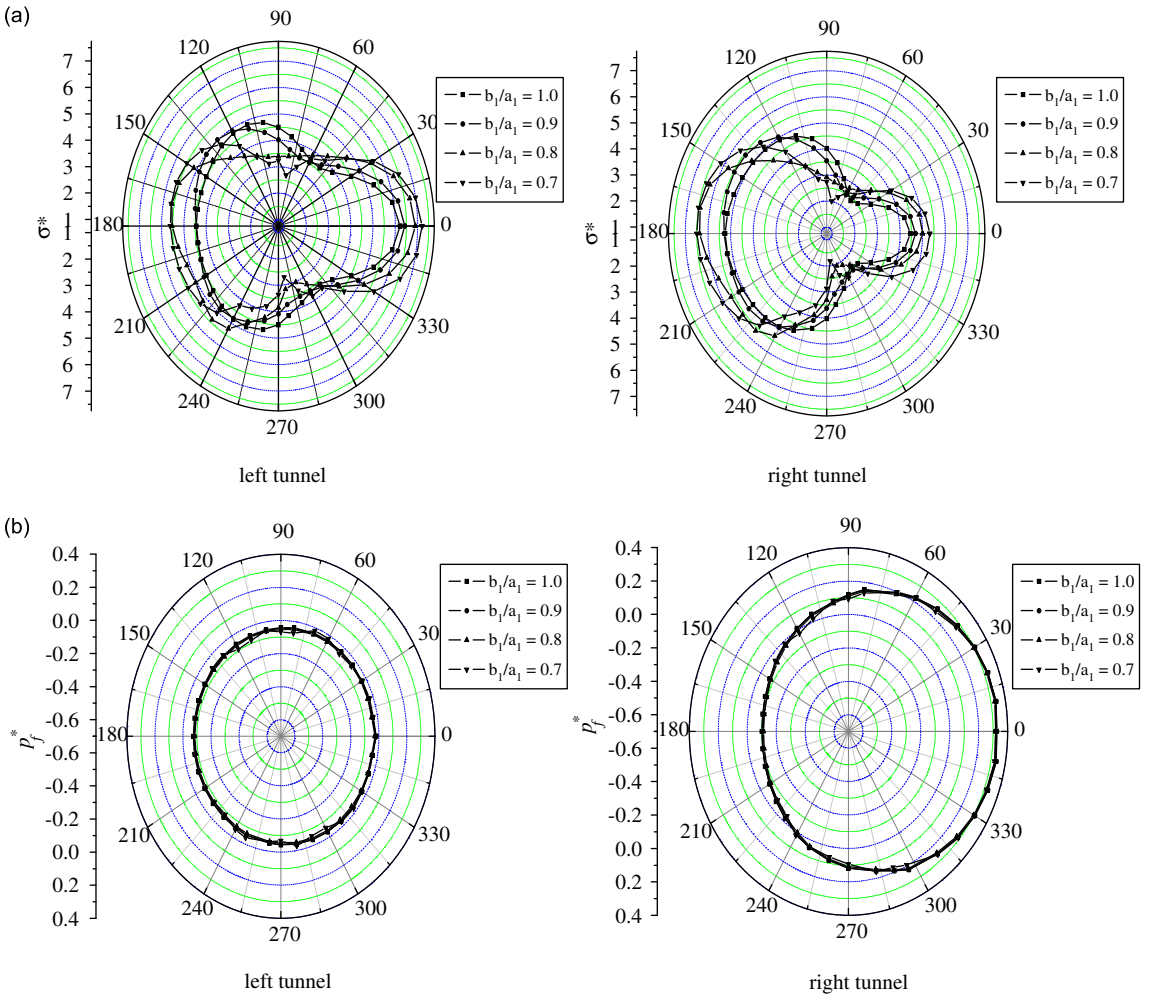

Fig. 3. Dynamic response of a pair of lined tunnels subject to an incidence P_1 wave with $\mathrm{Re}(k_f a) = 0.1$; $a_2/a_1 = 1.2$; $\delta/a_1 = 3.0$: (a) dimensionless stress σ^*; (b) dimensionless pore pressure p_f^*.

$$E^4_{13in} = \mathrm{i}\mu_{II}k_s^2 H^{(1)}_{n-2}(k_s|\zeta_{ij}|)\left(\frac{\zeta_{ij}}{|\zeta_{ij}|}\right)^{n-2} \mathrm{e}^{2\mathrm{i}\gamma_j} \tag{72c}$$

$$E^4_{14in} = \mathrm{i}\mu_{II}k_s^2 H^{(2)}_{n-2}(k_s|\zeta_{ij}|)\left(\frac{\zeta_{ij}}{|\zeta_{ij}|}\right)^{n-2} \mathrm{e}^{2\mathrm{i}\gamma_j} \tag{72d}$$

$$E^4_{21in} = \mu_{II}k_p^2 H^{(1)}_{n+2}(k_p|\zeta_{ij}|)\left(\frac{\zeta_{ij}}{|\zeta_{ij}|}\right)^{n+2} \mathrm{e}^{-2\mathrm{i}\gamma_j} \tag{72e}$$

$$E^4_{22in} = \mu_{II}k_p^2 H^{(2)}_{n+2}(k_p|\zeta_{ij}|)\left(\frac{\zeta_{ij}}{|\zeta_{ij}|}\right)^{n+2} \mathrm{e}^{-2\mathrm{i}\gamma_j} \tag{72f}$$

$$E^4_{23in} = -\mathrm{i}\mu_{II}k_s^2 H^{(1)}_{n+2}(k_s|\zeta_{ij}|)\left(\frac{\zeta_{ij}}{|\zeta_{ij}|}\right)^{n+2} \mathrm{e}^{-2\mathrm{i}\gamma_j} \tag{72g}$$

$$E^4_{24in} = -\mathrm{i}\mu_{II}k_s^2 H^{(2)}_{n+2}(k_s|\zeta_{ij}|)\left(\frac{\zeta_{ij}}{|\zeta_{ij}|}\right)^{n+2} \mathrm{e}^{-2\mathrm{i}\gamma_j} \tag{72h}$$

$$r^4_{1j} = 0 \tag{73a}$$

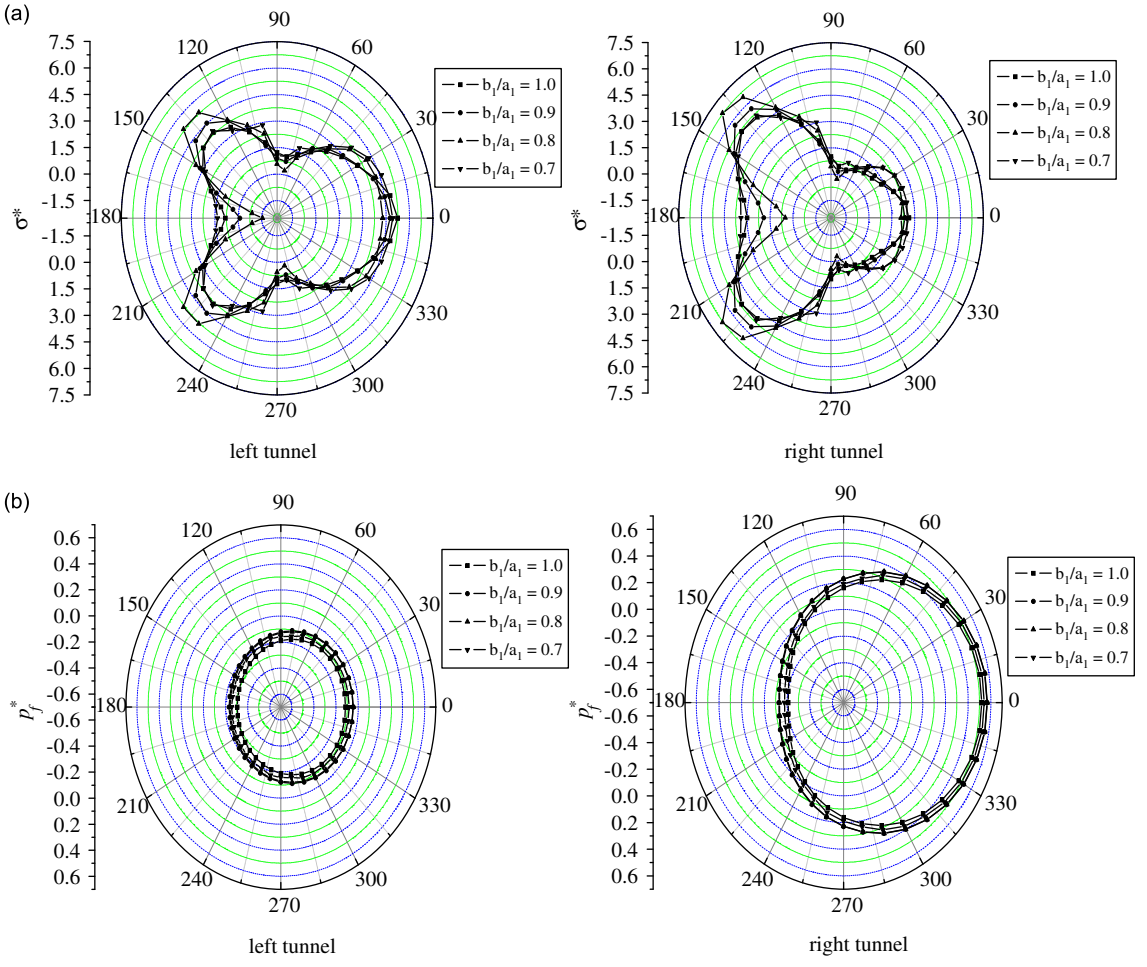

Fig. 4. Dynamic response of a pair of lined tunnels subject to an incidence P_1 wave with $\mathrm{Re}(k_f a) = 0.2$; $a_2/a_1 = 1.2$; $\delta/a_1 = 3.0$: (a) dimensionless stress σ^*; (b) dimensionless pore pressure p_f^*.

$$r_{2j}^{4} = 0 \tag{73b}$$

Multiplying both sides of Eq. (71) with $e^{-is\theta}$, and integrating over the interval $[-\pi, \pi]$ yields

$$\sum_{p=1}^{4}\sum_{i=1}^{2}\sum_{n=-\infty}^{n=\infty} E_{kpin}^{4s} x_{pin} = r_{kj}^{4s} \quad (k,j=1,2) \quad (s=0,\pm1,\pm2,\ldots) \tag{74}$$

where

$$E_{kpin}^{4s} = \frac{1}{2\pi}\int_{-\pi}^{\pi} E_{kpin}^{4} e^{-is\theta}\, d\theta \quad (s=0,\pm1,\pm2,\ldots) \tag{75}$$

$$r_{kj}^{4s} = \frac{1}{2\pi}\int_{-\pi}^{\pi} r_{kj}^{4} e^{-is\theta}\, d\theta \quad (s=0,\pm1,\pm2,\ldots) \tag{75b}$$

Eqs. (59), (64), (69) and (74) form a set of infinite algebraic equations for determining the constants a_{jn}, b_{jn}, c_{jn}, d_{jn}, e_{jn}, m_{jn}, n_{jn}. It should be pointed out that the above equations are all in infinite sums, therefore, the system of equations must be solved by truncating the infinite terms into the finite terms.

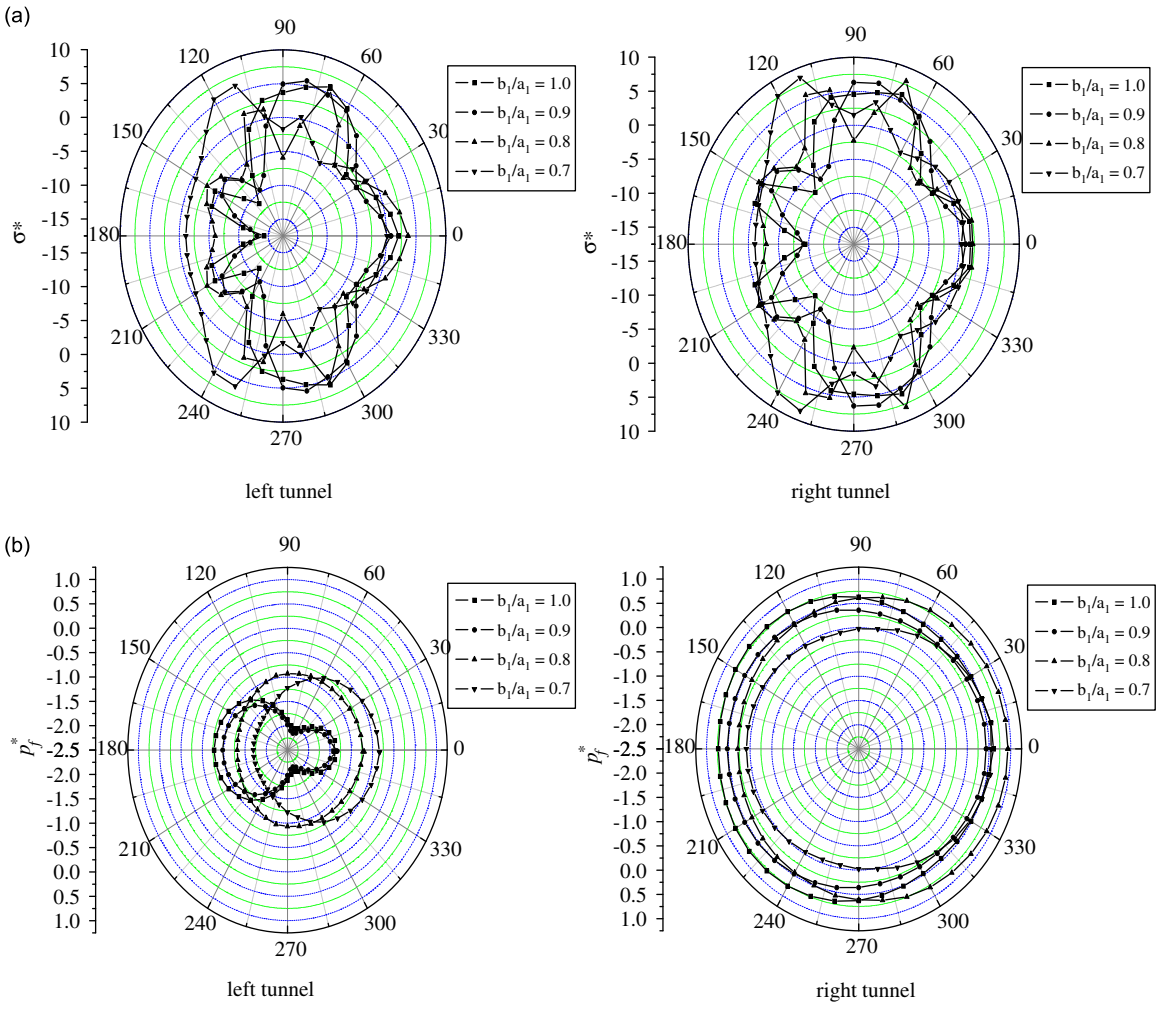

Fig. 5. Dynamic response of a pair of lined tunnels subject to an incidence P_1 wave with $\mathrm{Re}(k_f a) = 0.6$; $a_2/a_1 = 1.2$; $\delta/a_1 = 3.0$: (a) dimensionless stress σ^*; (b) dimensionless pore pressure p_f^*.

5. Numerical results

In the frequency domain, the harmonic incident plane P_1 wave can be written as

$$\varphi_f^{(I)} = \varphi_0 \exp[\mathrm{i}k_f(x\cos\beta + y\sin\beta)]\mathrm{e}^{-\mathrm{i}\omega t} = \varphi_0 \exp\left[\frac{\mathrm{i}k_f}{2}(\bar{z}e^{\mathrm{i}\beta} + ze^{-\mathrm{i}\beta})\right]\mathrm{e}^{-\mathrm{i}\omega t} \tag{76}$$

where β denotes the incident angle; φ_0 represents the potential amplitude for the incident P_1 wave. The dynamic stress concentration factor σ^* is defined as the ratio of the tangential effective stress along the boundary of the tunnel to the normal effective stress of the incident wave at the wave front passing through the origin.

$$\sigma^* = \frac{\sigma_{\tilde{y}}}{\sigma_0} \tag{77}$$

where

$$\sigma_0 = \mathrm{Re}[-(\lambda + 2\mu)k_f^2\varphi_0] \tag{78}$$

For the case of impermeable condition, the pore pressure concentration factor is defined as the ratio of the pore pressure along the boundary of the lined tunnel to the pore pressure of the incident wave at the wave front passing through the origin.

$$p_f^* = \frac{p_f}{p_{f0}} \tag{79}$$

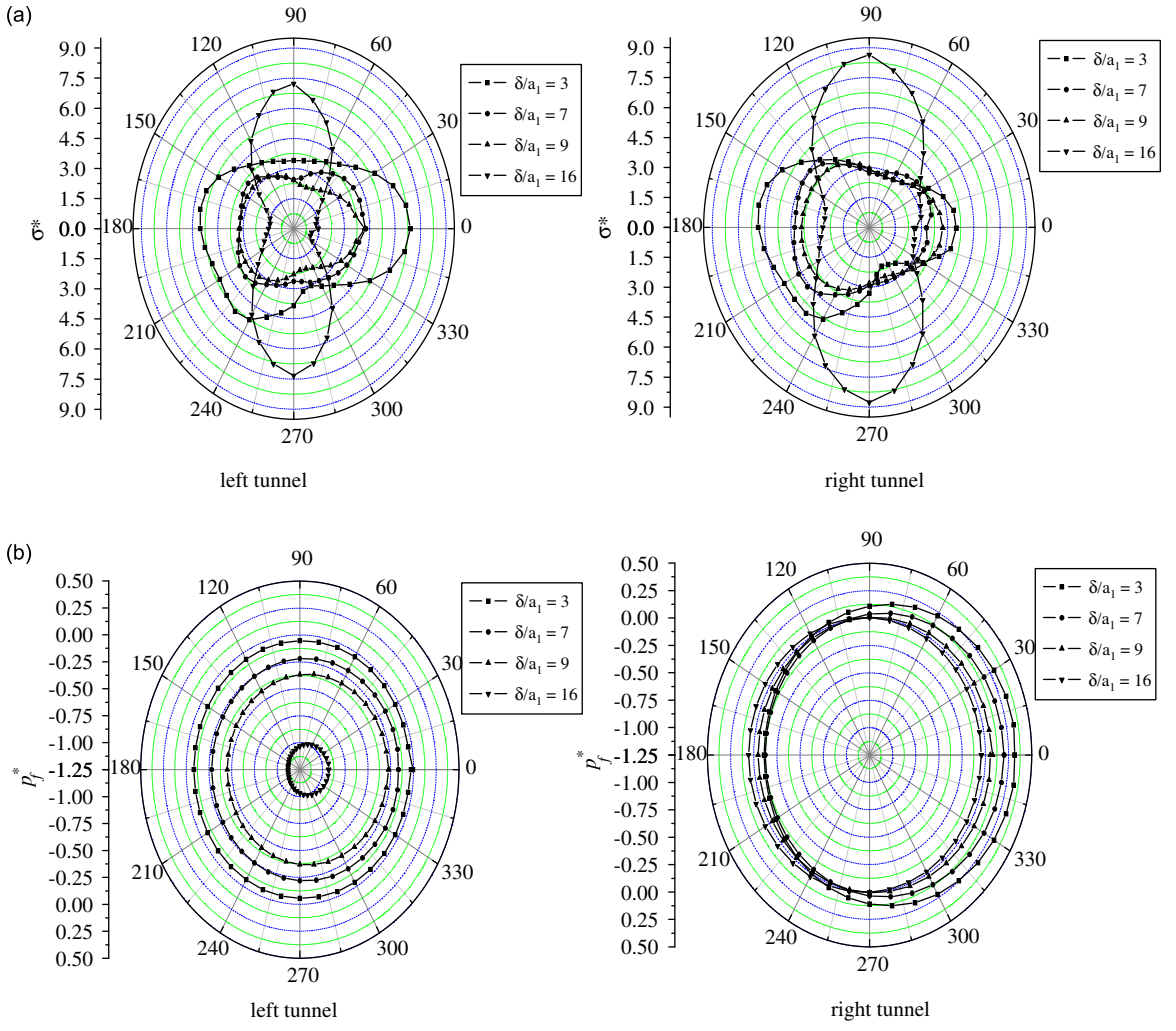

Fig. 6. Dynamic response of a pair of lined tunnels subject to an incidence P_1 wave with $\mathrm{Re}(k_f a) = 0.1$; $a_2/a_1 = 1.2$; $b_1/a_1 = 0.8$: (a) dimensionless stress σ^*; (b) dimensionless pore pressure p_f^*.

where

$$p_{f0} = \mathrm{Re}[-A_f k_f^2 \varphi_0] \tag{80}$$

First, the convergence of the proposed scheme will be verified. Then, the dynamic response of a pair of lined tunnels to seismic wave with selected the dimensionless wavenumber, elliptic ratio, thickness of liner and distance between two tunnels parameter will be calculated as numerical examples.

5.1. Convergence tests

In this example, the response of a pair of lined tunnels subject to seismic wave is used to check the convergence of the proposed approach. The input parameter values for the porous medium and the liner are compiled in Table 1. The incident angle is $\beta = 0^\circ$; the elliptic ratio $b_1/a_1 = 1.0$; the thickness of the liner $a_2/a_1 = 1.1$; the distance of two tunnels $\delta/a_1 = 3.0$; the dimensionless wavenumber $\mathrm{Re}(k_f a) = 0.1, 0.2, 0.3$; the number of terms in series solution N takes 6, 7, 8 and 9.

The stresses and the pore pressures around the right tunnel are given when the dimensionless wavenumber $\mathrm{Re}(k_f a) = 0.1, 0.2, 0.3$. Fig. 2 shows that the stresses converge much slower than the pore pressures. For the number of terms in series solution N takes 8 and 9, the stresses and the pore pressures have a good convergence. Therefore, the number of terms truncated from the infinite series N is takes as 8 for each part of numerical results.

5.2. Dynamic response of a pair of tunnels with different dimensionless wavenumber and elliptic ratio

The elliptic ratio is represented by the ratio of the short axial radius to the long axial radius b_1/a_1. The input parameter values of the porous medium and the liner use in Table 1. The most important incident angle is $\beta = 0^\circ$ (end-on), as it

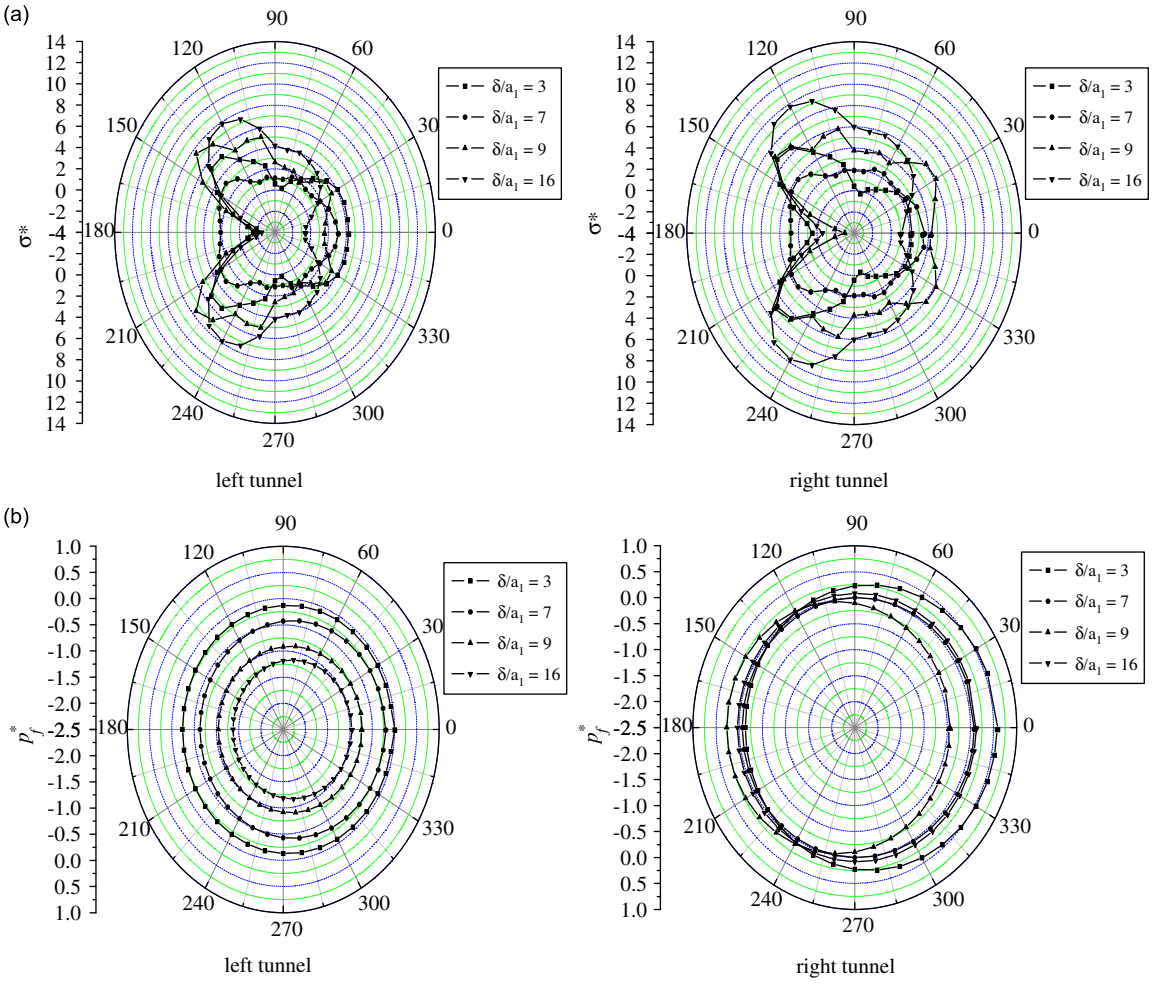

Fig. 7. Dynamic response of a pair of lined tunnels subject to an incidence P_1 wave with $\mathrm{Re}(k_f a) = 0.2$; $a_2/a_1 = 1.2$; $b_1/a_1 = 0.8$: (a) dimensionless stress σ^*; (b) dimensionless pore pressure p_f^*.

best helps to expose the physics of the problem. Here, the dynamic response of a pair of lined tunnels to P_1 wave with different elliptic ratio and dimensionless wavenumber will be calculated as a numerical example. Figs. 3–5 show the stress amplitudes and the pore pressure amplitudes at the surface of two tunnels at selected dimensionless wavenumber ($\mathrm{Re}(k_f a) = 0.1, 0.2, 0.6$) and elliptic ratio ($b_1/a_1 = 1.0, 0.9, 0.8, 0.7$), distance between two tunnels $\delta/a_1 = 3.0$. Careful examination of Figs. 3–5 reveal some interesting features of the problem. The most important observations are as follows. For the lower dimensionless wavenumber $\mathrm{Re}(k_f a) = 0.1$ (Fig. 3), the only very small difference of the pore pressures are observed when changing elliptic ratio b_1/a_1. However, for the stresses, the difference is observable when changing elliptic ratio. The stresses increase with decreasing elliptic ratio b_1/a_1. As the dimensionless wavenumber $\mathrm{Re}(k_f a)$ is increased to 0.2 (Fig. 4), the stress amplitudes increase when elliptic ratio b_1/a_1 decreasing from 1.0 to 0.8. The pore pressures have small difference with decreasing elliptic ratio b_1/a_1 from 1.0 to 0.7. For the higher dimensionless wavenumber $\mathrm{Re}(k_f a) = 0.6$ (Fig. 5), the elliptic ratio have a significance influence on the dynamic stresses and the pore pressures. Figs. 3–5 indicate the multiple scattering and the wave interaction effect increase when increasing wavenumber.

5.3. Dynamic response of a pair of tunnels with different dimensionless wavenumber and distance between two tunnels

To further assess the multiple scattering and the interaction effect, Figs. 6 and 7 show the distribution of the stress amplitudes and the pore pressure amplitudes at the surface of two tunnels for incident P_1 wave at selected dimensionless wavenumber ($\mathrm{Re}(k_f a) = 0.1, 0.2$) and distance between two tunnels ($\delta/a_1 = 3, 7, 9, 16$). The input parameter values of the porous medium and the liner use in Table 1. Comments similar to the previous case can readily be made.

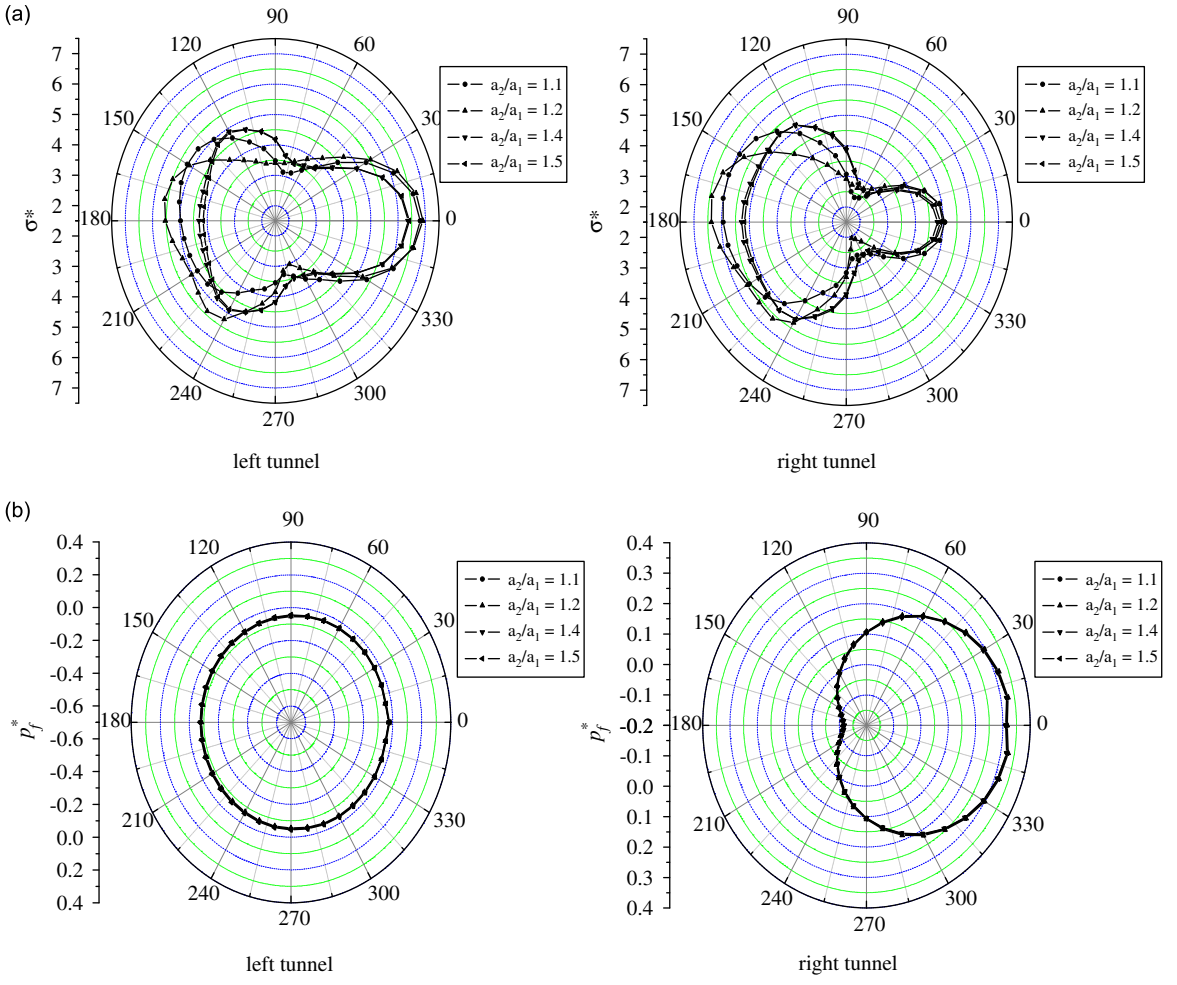

Fig. 8. Dynamic response of a pair of lined tunnels subject to an incidence P_1 wave with $\mathrm{Re}(k_f a) = 0.1$; $\delta/a_1 = 3$; $b_1/a_1 = 0.8$: (a) dimensionless stress σ^*; (b) dimensionless pore pressure p_f^*.

The main distinction is that the multiple scattering and the interaction effect nearly vanish, as the distance between two tunnels increase to $\delta/a_1 = 16$. For the lower wavenumber $\mathrm{Re}(k_f a) = 0.1$ (Fig. 6), the stresses decrease when distances between two tunnels increase from $\delta/a_1 = 3$ to $\delta/a_1 = 9$. When distance arrive to $\delta/a_1 = 16$, the stress contribution of two tunnels is similar to that of single tunnel. The pore pressures decrease when increasing distances between two tunnels. For the wavenumber $\mathrm{Re}(k_f a) = 0.2$ (Fig. 7), the largest of the stresses occur at $\delta/a_1 = 16$ and the smallest of the stresses occur at $\delta/a_1 = 7$. The stresses for the case $\delta/a_1 = 9$ is larger than that for the case $\delta/a_1 = 3$. For the left tunnel, the pore pressures decrease with increasing distances between two tunnels δ/a_1. For the right tunnel, the largest of the pore pressures occur at $\delta/a_1 = 3$ and the smallest of the pore pressures occur at $\delta/a_1 = 9$.

5.4. Dynamic response of a pair of tunnels with different thickness of liner and distance between two tunnels

Finally, we check the stress amplitudes and the pore pressure amplitudes for incidence P_1 wave at selected thickness of liner ($a_2/a_1 = 1.1, 1.2, 1.4, 1.5$) and distance between two tunnels $\delta/a_1 = 3, 9, 16$. The input parameter values of the porous medium and the liner use in Table 1. Figs. 8–10 show the difference of the stresses is more pronounced than the pore pressures when increasing thicknesses of liner. Figs. 8–10 indicate the pore pressures have no obviously change when increasing thicknesses of liner. Figs. 8 and 10 show that the largest of the stresses occurs at $a_2/a_1 = 1.2$ and the smallest of the stresses occurs at $a_2/a_1 = 1.4$ and 1.5 for distances between two tunnels $\delta/a_1 =$ 3 and 16. Fig. 9 shows that the largest of the stresses occurs at $a_2/a_1 = 1.4$ and the smallest of the stresses occurs at $a_2/a_1 = 1.5$ for distances between two tunnels $\delta/a_1 = 9$.

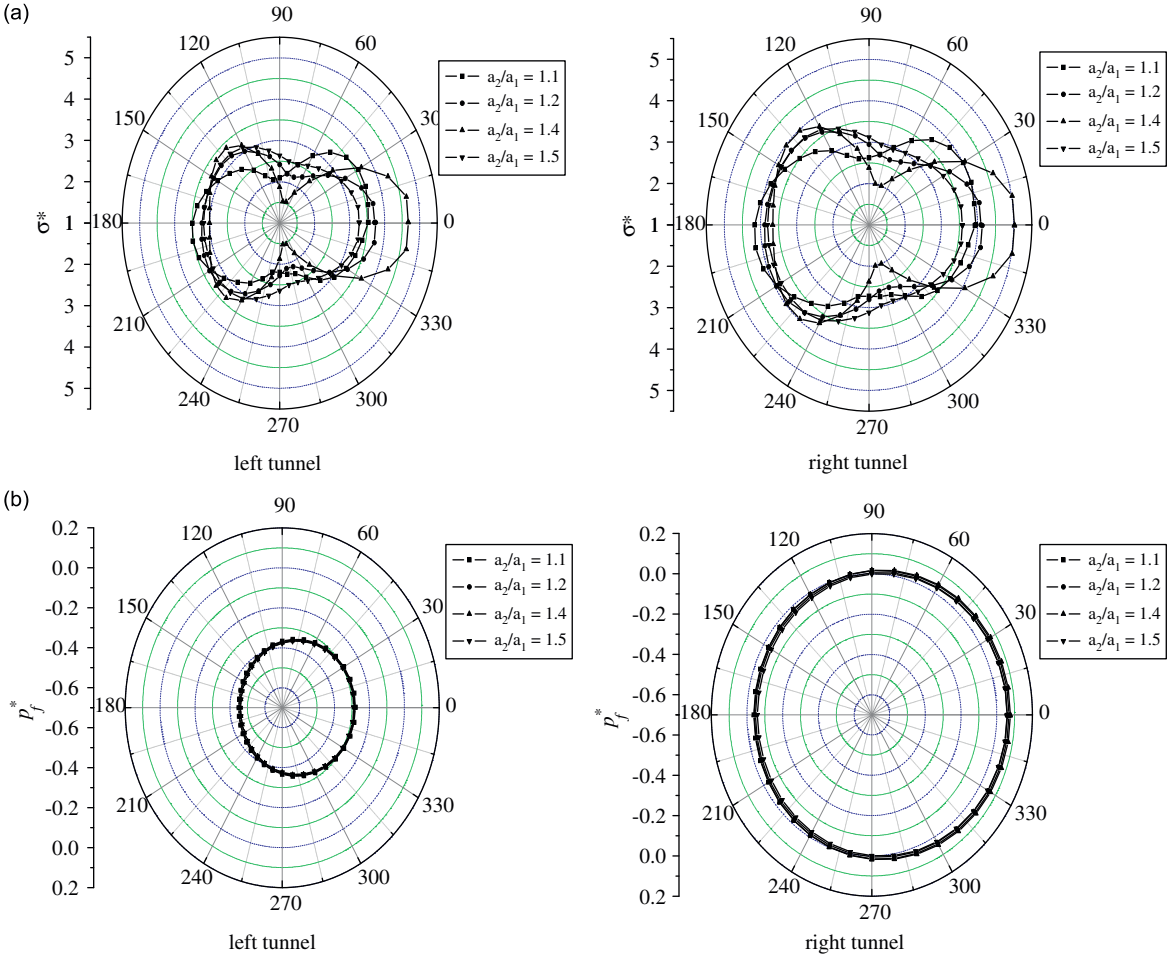

Fig. 9. Dynamic response of a pair of lined tunnels subject to an incidence P_1 wave with $\mathrm{Re}(k_f a) = 0.1$; $\delta/a_1 = 9$; $b_1/a_1 = 0.8$: (a) dimensionless stress σ^*; (b) dimensionless pore pressure p_f^*.

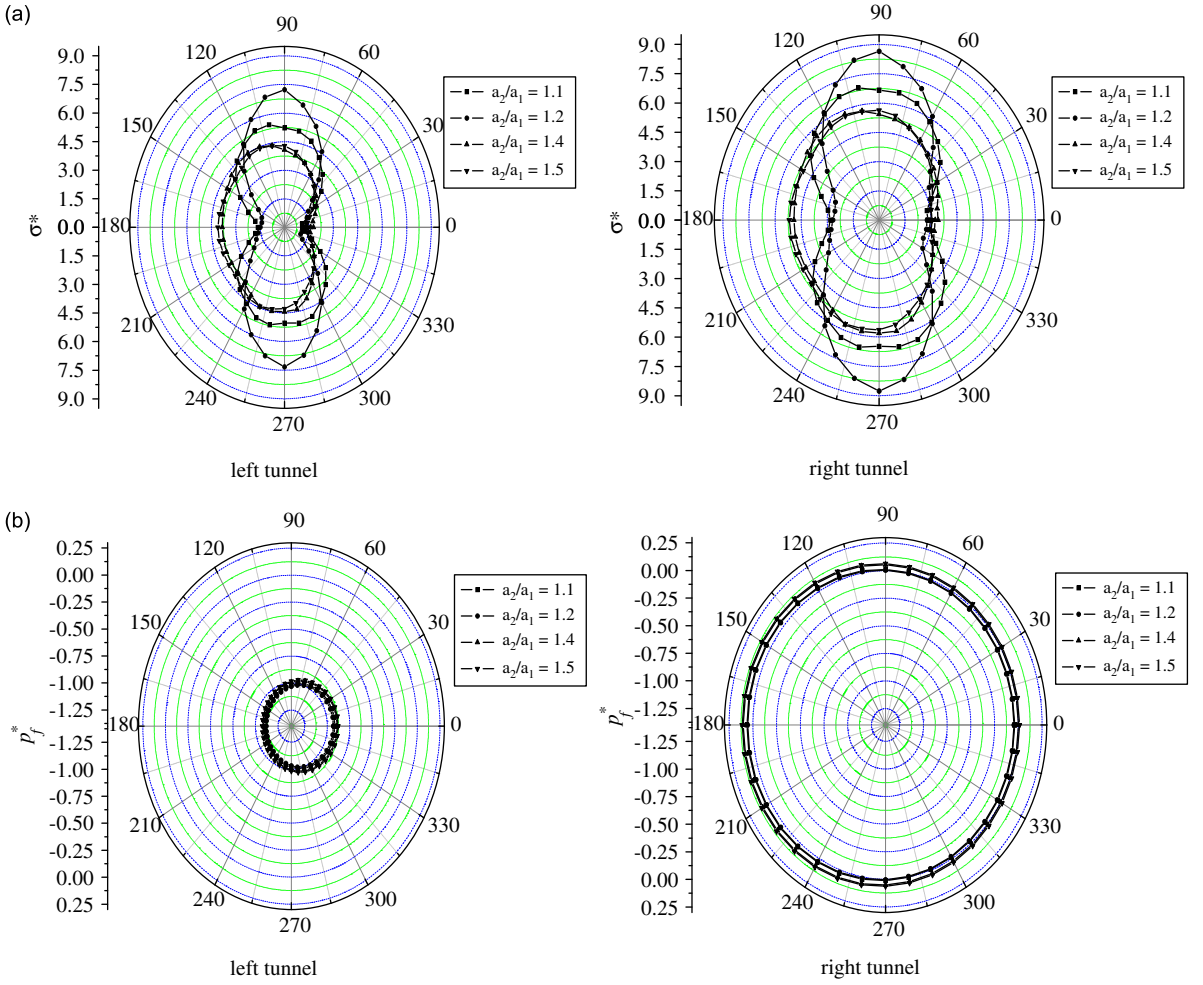

Fig. 10. Dynamic response of a pair of lined tunnels subject to an incidence P_1 wave with $\mathrm{Re}(k_f a) = 0.1$; $\delta/a_1 = 16$; $b_1/a_1 = 0.8$: (a) dimensionless stress σ^*; (b) dimensionless pore pressure p_f^*.

6. Conclusion

The complex variable function method and the wave function expansion method are used to develop a semi-analytical solution for the problem of the dynamic interaction between a pair of elliptic lined tunnels in a poroelastic medium. The primary objectives are to investigate the multiple scattering and the interaction effect between two tunnels. Based on the derivation and numerical examples presented above, the following conclusions are drawn:

(1) Numerical results show that the complex variable function method and the wave function expansion method can be used in the calculation of lined tunnels embedded in a porous medium and subjected to plane harmonic wave. The convergence of the method has been examined numerically and a good convergence has been observed in the calculation.
(2) The numerical results include the dynamic stresses and the pore pressures of a pair of tunnels at selected wavenumber, thickness, elliptic ratio and distance parameters. The numerical results show that the wavenumber, thickness of liner, elliptic ratio and distance of two tunnels has a significance influence on the dynamic stresses and the pore pressures.
(3) The multiple scattering and the interaction effect at two lined tunnels are fairly pronounced, in particular, when the tunnels are closely located. The influence of the multiple scattering and the multiple interactions between two tunnels on the stresses becomes more observable with the decreasing distance between the two tunnels.

Acknowledgement

The research was financially supported by Shanghai Leading Academic Discipline Project, Project Number: B208.

Reference

[1] N.R. Zitron, Multiple scattering of elastic waves by two arbitrary cylinders, *Journal of the Acoustical Society of America* 42 (1967) 620–624.
[2] V.E. Glazanov, E.L. Shenderov, Plane wave scattering by cylindrical cavity in isotropic elastic medium, *Soviet Physics Acoustics* 17 (1971) 41–43.
[3] V.V. Varadan, Scattering matrix for elastic waves, II, application to elliptic cylinders, *Journal of the Acoustical Society of America* 63 (1978) 1014–1024.
[4] V.W. Lee, M.D. Trifunac, Response of tunnels to incident SH-waves, *Journal of Engineering Mechanics, ASCE* 105 (1979) 643–659.
[5] Y.L. Chen, The analysis of elastic liner in a cylindrical tunnel subjected to SH-waves, *Journal of the Chinese Institute of Engineers* 3 (1980) 21–29.
[6] N.N. Fotieva, Determination of the minimum seismically safe distance between two parallel tunnels, *Soil Mechanics and Foundation Engineering* 17 (1980) 111–116.
[7] S. Sancar, Y.H. Pao, Spectral analysis of elastic pulses back scattered from two cylindrical cavities in a solid, *Journal of the Acoustical Society of America* 69 (1981) 1591–1596.
[8] S.K. Datta, K.C. Wong, A.H. Shah, Dynamic stress and displacement around cylindrical cavities of arbitrary shapes, *Journal of Applied Mechanics, ASME* 51 (1984) 798–803.
[9] X. Zeng, A.S. Cakmak, Scattering of plane SH-waves by multiple cavities, *American Society of Mechanical Engineers* 98 (1985) 155–163.
[10] N. Moeen-Vaziri, M.D. Trifunac, Scattering and diffraction of plane P and SV waves by two-dimensional inhomogeneities: part II, *Soil Dynamics and Earthquake Engineering* 7 (1988) 189–200.
[11] C.P. Providakis, D.A. Sotiropoulos, D.E. Beskos, BEM analysis of reduced dynamic stress-concentration by multiple holes, *Communications in Numerical Methods in Engineering* 9 (1993) 917–924.
[12] S.X. Shi, F. Han, Z.Q. Wang, D.K. Liu, The interaction of plane SH waves and non-circular cavity surfaced with lining in anisotropic media, *Journal of Applied Mathematics and Mechanics* 17 (1996) 855–867.
[13] A.A. Stamos, D.D. Theodorakopoulos, D.E. Beskos, Harmonic wave response of tunnels in poroelastic saturated soil, *Advances in Earthquake Engineering* 2 (1995) 101–112.
[14] C.A. Davis, V.W. Lee, J.P. Bardet, Transverse response of underground cavities and pipes to incident SV waves, *Earthquake Engineering and Structural Dynamics* 30 (2001) 383–410.
[15] M. Eisenberger, E. Efraim, In-plane vibrations of shear deformable curved beam, *International Journal for Numerical Methods in Engineering* 52 (2001) 1221–1234.
[16] T. Okumura, N. Takewaki, K. Shimizu, K. Fukutake, Dynamic response of twin circular tunnels during earthquakes, *NIST Special Publication* 840 (1992) 181–191.
[17] I.D. Moore, F. Guan, Three-dimensional dynamic response of lined tunnels due to incident seismic waves, *Earthquake Engineering and Structural Dynamics* 25 (1996) 357–369.
[18] P. Rembert, H. Franklin, J.M. Conoir, Multichannel resonant scattering theory applied to a fluid-filled cylindrical cavity in an elastic medium, *Wave Motion* 40 (2004) 277–293.
[19] H. Rhee, Y. Park, New analysis of elastic wave resonance scattering from a fluid-filled cylindrical cavity, *JSME International Journal Series C: Mechanical Systems Machine Elements Manufacturing* 47 (2004) 297–304.
[20] S. Robert, J.M. Conoir, H. Franklin, F. Luppé, Resonant elastic scattering by a finite number of cylindrical cavities in an elastic matrix, *Wave Motion* 3 (2004) 225–239.
[21] C.C. Mei, B.I. Si, D.Y. Cai, Scattering of simple harmonic waves by a circular cavity in a fluid-filled treated poro-elastic medium, *Wave Motion* 6 (1984) 265–278.
[22] V.N. Krutin, M.G. Markov, A.Y. Yumatov, Normal waves in a fluid-filled cylindrical cavity located in a saturated porous medium, *Journal of Applied Mathematics and Mechanics* 52 (1988) 67–74.
[23] C. Zimmerman, Scattering of plane compressional waves by spherical inclusions in a poroelastic medium, *Journal of the Acoustical Society of America* 94 (1993) 527–536.
[24] T. Senjuntichat, R.K.N.D. Rajapakse, Transient response of a circular cavity in a poroelastic medium, *International Journal for Numerical and Analytical Methods in Geomechanics* 17 (1993) 357–383.
[25] Y.Y. Hu, L.Z. Wang, Y.M. Chen, S.M. Wu, Z.M. Zhang, Scattering and refracting of plane strain wave by a cylindrical inclusion in fluid-saturated soils, *Acta Seismologica Sinica* 11 (1998) 355–363.
[26] C.H. Lin, V.W. Lee, M.D. Trifunac, On the reflection of elastic waves in a poroelastic half-space saturated with non-viscous fluid, Report CE01-04 Department of Civil Engineering University of Southern California, 2001.
[27] S.E. Kattis, D.E. Beskos, A.H.D. Cheng, 2D dynamic response of unlined and lined tunnels in poroelastic soil to harmonic body waves, *Earthquake Engineering and Structural Dynamics* 32 (2003) 97–110.
[28] B. Gatmiri, H. Eslami, Wave scattering in cross-anisotropic porous media around the cavities and inclusions, *Soil Dynamics and Earthquake Engineering* 28 (2008) 1014–1027.
[29] J.F. Lu, J.H. Wang, The scattering of elastic waves by holes of arbitrary shapes in saturated soil, *Acta Mechanica Sinica* 34 (2002) 904–914.
[30] J.H. Wang, X.L. Zhou, J.F. Lu, Dynamic stress concentration around elliptic cavities in saturated poroelastic soil under harmonic plane waves, *International Journal of Solids and Structures* 42 (2005) 4295–4310.
[31] J.F. Lu, D.S. Jeng, T.L. Lee, Dynamic response of a piecewise circular tunnel embedded in a poroelastic medium, *Soil Dynamics and Earthquake Engineering* 27 (2007) 875–891.
[32] S.M. Hasheminejad, R. Avazmohammadi, Harmonic wave diffraction by two circular cavities in a poroelastic formation, *Soil Dynamics and Earthquake Engineering* 27 (2007) 29–41.
[33] M.A. Biot, Theory of propagation of elastic waves in a fluid-saturated porous solid, I, low frequency range, *Journal of the Acoustical Society of America* 28 (1956) 168–178.
[34] M.A. Biot, Mechanics of deformation and acoustic propagation in porous media, *Journal of Applied Mathematics and Mechanics* 33 (1962) 1482–1498.